THREE-DIMENSIONAL ANALYSIS OF THE TEMPERATURE AND VELOCITY FIELDS IN CYLINDRICAL THERMAL TANKS

Darci Luiz Savicki
Mechanical Engineering Graduate Program – UFRGS. Rua Sarmento Leite, 425, 90050-170 - Porto Alegre, RS, Brazil.
darcilus@mecanica.ufrgs.br

Horácio A. Vielmo
Department of Mechanical Engineering – UFRGS. Rua Sarmento Leite, 425, 90050-170 - Porto Alegre, RS, Brazil.
vielmoh@mecanica.ufrgs.br

Arno Krenzinger
Mechanical Engineering Graduate Program – UFRGS. Rua Sarmento Leite, 425, 90050-170 - Porto Alegre, RS, Brazil.
arno@mecanica.ufrgs.br

Abstract. *A three-dimensional numerical investigation of the laminar natural convection in cylindrical thermal tanks, by the numerical simulation using the Finite Volumes Method, in structured mesh is presented. The 3D algorithm used in this study is validated based on experimental data available in literature, for the case of a cylindrical vertical tank. This algorithm is then used to simulate a horizontal cylindrical vertical tank. The formation of thermal and hydrodynamic boundary layers, and the consequent formation of a stratified temperature profile in the vertical direction were verified. The average fluid temperature, and internal metal wall storage tank average temperature were defined for calculation of the Nusselt and Rayleigh numbers. The transient solution of the temperature and velocity fields showed the formation of "fringes" by the radial wall, which was more pronounced on the top region of the storage tank.*

Keywords: Storage tanks, Natural convection, Finite Volumes Method, Three-dimensional numerical investigation.

1. Introduction

In the presence of the gravitational field, the variation of the specific mass of a fluid due to a non-uniform temperature field determines the emergence of buoyancy forces. The resulting fluid movement, known as natural convection, becomes important in many technical applications involving non-uniformly heated fluids, such as heating or cooling devices, solar energy collectors, crystal growth, and solidification processes, among others.

There are several theoretical and/or experimental studies on natural convection in rectangular or cylindrical cavities. Using mathematical modeling, many take into account some kind of symmetry that allows numerical simulation only in two dimensions. A recent example is the study of Oliveski *et al* (2003), which presents an experimental investigation and a theoretical study on the temperature fields and velocity inside vertical cylindrical thermal storage tanks under boundary conditions of the third kind. In this study, in order not to disrupt axis symmetry, the authors considered water entrance/exit at the axis.

In other geometries, a satisfactory description of natural convection requires the consideration of the three physical dimensions, such as when using a horizontal cylindrical thermal storage tank. In this case, even assuming symmetry, the calculation domain becomes three-dimensional. Only a few numerical studies on natural convection take into consideration geometries that require three-dimensional solutions. Some reasons for this are the lack of three-dimensional algorithms, the increase in the size of the equations to be solved, as well as the consequent increase in computational time, which rendered such simulations unfeasible until recently.

An example of three-dimensional numerical investigation is described by Schneider and Straub (1992), who considered the problem of laminar natural convection in an inclined cylinder with different axial wall temperatures and lateral insulation. In this study, the used grid is very poor, probably due to the computational limitations of that time. The authors concluded that, for the boundary conditions studied, with Pr=0.7 and H/D=1, maximum heat transfer occurs for the $\theta \approx 45º$-$60º$ angles. Later, using the CFX-F3D software, Xia *et al* (1998) simulated turbulent and laminar flow and heat transfer in a horizontal cylinder with heat flow prescribed in the walls, and validated their results with their own experimental data. The authors showed that, after reaching a stable regime, there is temperature stratification in vertical plans, and concluded that this stratification is limited by the hydrodynamic boundary layer along the walls. Rubinov *et al*. (2004) numerically studied the occurrence of three-dimensional instabilities in the natural convection flow in vertical cylinder with partially heated side wall and observed different modes of three-dimensional disturbances that alternate with the variation of aspect ratio.

Almost all studies found in literature assume boundary conditions of the first and second kind in the walls, and null wall thickness. There is a lack of studies considering heat transfer through boundary condition of the third kind, and that include in the calculation domain the walls of the storage tank. In order to complement the research mentioned above,

the present study presents a numerical study on temperature fields and velocity in a horizontal cylindrical thermal storage tank subjected to heat loss to the environment by boundary condition of the third kind. This situation occurs, for instance, in water heating systems using solar energy.

2. Physical and mathematical model

Figure 1 shows the geometry and the dimensions of the storage tank used in this simulation.

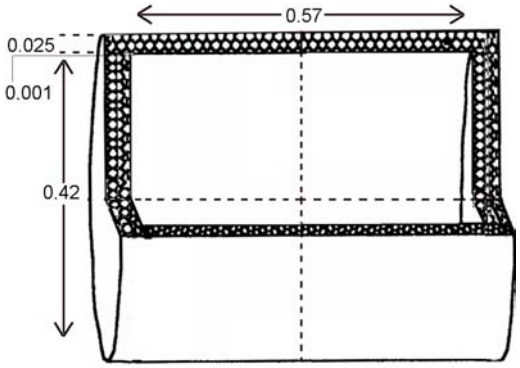

Figure 1 – Geometry and dimensions of the storage tank [m]

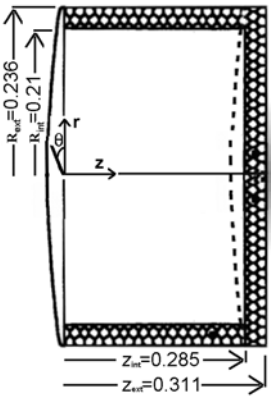

Figure 2 – Calculation domain [m]

It is assumed that the layers of the internal metallic wall and of the insulation have equal values in the radial and axial directions, being respectively e_{mw}=0.001m and e_{ins}=0.025m. The internal metallic wall is made of copper, and the insulation is polyurethane. It is initially considered that the tank is completely filled with water at a uniform temperature of T_{int}=50ºC, and that the environmental temperature is 15ºC. The tank then starts to transfer heat to the environment, which temperature remains constant at T_{ext}=15ºC. The solid region of the metallic wall and thermal insulation is assumed to be initially at an intermediate temperature ½ (T_{int}+ T_{ext}). The heat transfer coefficient used was h=10 W/m^{2}K. Taking into consideration two vertical symmetry plans, being one (r, θ) passing by the intermediate point of length z and the plan (r, z) passing by the diameter, the calculation domain that needs to be simulated is reduced to the regions shown in Fig. 2.

In cylindrical coordinates, using the approximation of Boussinesq, the problem can be described by the following system of equations:

Equation of continuity:

$$\frac{1}{r}\frac{\partial\left(rV_r\right)}{\partial r}+\frac{1}{r}\frac{\partial V_\theta}{\partial\theta}+\frac{\partial V_z}{\partial z}=0 \tag{1.1}$$

Equations of movement:

In the radial direction r:

$$\rho_\infty\left(\frac{\partial V_r}{\partial t}+V_r\frac{\partial V_r}{\partial r}+\frac{V_\theta}{r}\frac{\partial V_r}{\partial\theta}-\frac{V_\theta^2}{r}+V_z\frac{\partial V_r}{\partial z}\right)=$$
$$-\frac{\partial p_H}{\partial r}+\mu\left[\frac{\partial}{\partial r}\left(\frac{1}{r}\frac{\partial\left(rV_r\right)}{\partial r}\right)+\frac{1}{r^2}\frac{\partial^2V_r}{\partial\theta^2}-\frac{2}{r^2}\frac{\partial V_\theta}{\partial\theta}+\frac{\partial^2V_r}{\partial z^2}\right]+\rho_\infty\beta\left(T-T_\infty\right)g\cos\theta \tag{1.2}$$

In the angular direction θ:

$$\rho_\infty\left(\frac{\partial V_\theta}{\partial t}+V_r\frac{\partial V_\theta}{\partial r}+\frac{V_\theta}{r}\frac{\partial V_\theta}{\partial\theta}-\frac{V_rV_\theta}{r}+V_z\frac{\partial V_\theta}{\partial z}\right)=$$
$$-\frac{\partial p_H}{\partial\theta}+\mu\left[\frac{\partial}{\partial r}\left(\frac{1}{r}\frac{\partial\left(rV_\theta\right)}{\partial r}\right)+\frac{1}{r^2}\frac{\partial^2V_\theta}{\partial\theta^2}+\frac{2}{r^2}\frac{\partial V_r}{\partial\theta}+\frac{\partial^2V_\theta}{\partial z^2}\right]-\rho_\infty\beta\left(T-T_\infty\right)g\,sen\theta \tag{1.3}$$

In the axial direction z:

$$\rho_\infty\left(\frac{\partial V_z}{\partial t}+V_r\frac{\partial V_z}{\partial r}+\frac{V_\theta}{r}\frac{\partial V_z}{\partial\theta}+V_z\frac{\partial V_z}{\partial z}\right)=$$
$$-\frac{\partial p_H}{\partial z}+\mu\left[\frac{1}{r}\frac{\partial}{\partial r}\left(r\frac{\partial V_z}{\partial r}\right)+\frac{1}{r^2}\frac{\partial^2V_z}{\partial\theta^2}+\frac{\partial^2V_z}{\partial z^2}\right] \tag{1.4}$$

Initial conditions: For the complete domain: $V_\theta = V_r = V_z = 0$

Boundary conditions: In the entire insulation and metallic wall region: $V_\theta = V_r = V_z = 0$

In the line r=0: $V_\theta = V_r = 0, \frac{V_z}{\partial r} = 0$

In the symmetry plan (r, z), where θ=0 and θ=π: $\frac{\partial V_r}{\partial \theta} = \frac{\partial V_z}{\partial \theta} = V_\theta = 0$

In the symmetry plan (r, θ), where z=0: $\frac{\partial V_\theta}{\partial z} = \frac{\partial V_r}{\partial z} = V_z = 0$

Equation of energy:

$$\rho_\infty c_p \left(\frac{\partial T}{\partial t} + V_r \frac{\partial T}{\partial r} + \frac{V_\theta}{r} \frac{\partial T}{\partial \theta} + V_z \frac{\partial T}{\partial z} \right) = k \left[\frac{1}{r} \frac{\partial}{\partial r} \left(r \frac{\partial T}{\partial r} \right) + \frac{1}{r^2} \frac{\partial^2 T}{\partial \theta^2} + \frac{\partial^2 T}{\partial z^2} \right] + S^T \qquad (1.5)$$

Initial conditions: In the interior condition : $T=T_{int}$

In the region of thermal insulation and metallic wall: $T=1/2(T_{int}+T_{ext})$

Boundary conditions:

In the r line =0: $\frac{\partial T}{\partial \theta} = 0$

In the symmetry plan (r, z), where θ=0 and θ=π: $\frac{\partial T}{\partial \theta} = 0$

In the symmetry plan (r, θ), where z=0: $\frac{\partial T}{\partial z} = 0$

In the boundaries $r=R_{ext}$ and $z=Z_{ext}$: h and T_∞ prescribed.

2.1. Solution method

In the development of the computational code, were incorporated some routines of the general purpose code of Patankar (1972). The velocity-pressure coupling algorithm SIMPLE was used. For the solution of the resulting equation system, the TDMA was employed, with block correction in some equations. The interpolation function for the advective terms was the Power-law. The code was extensively tested in other problem situations, and it was verified that it produces results according to theoretical and experimental results found in literature. For the case studied here, the authors are not aware of the existence of numerical or experimental data. When discretizing the calculation domain for the fluid region in the radial and axial directions, non-uniform refinement is applied, thereby concentrating more volumes by the wall, in order to obtain information on the thermal and hydrodynamic limit layers. For numerical reasons, refinement is also applied by the central axis for the radial direction. One further volume is used in the radial and axial directions for the metallic wall, and two volumes for the thermal insulation layer. In the angular direction, discretization with uniform spacing is employed. Taking into account the volume referring to the metallic wall, and the two volumes referring to the thermal insulation layer, the grid is 40 x 40 x 40 in directions (r, θ, z), which corresponds to a system with 64000 equations. Fig. 3 shows a view of the calculation domain.

The equations were iteratively solved at each step of time of 1 second in order to reach the criteria of convergence for the thermal and hydrodynamic fields. The criterion was $\frac{T^{n+1} - T^n}{T^n} \leq 10^{-6}$ for the thermal field and $SMAX \leq 10^{-6}$ for the hydrodynamic field, which means that matter created/destroyed in each volume to satisfy the equation of continuity is below 10^{-6} kg/m^3.

In order to establish the number of Rayleigh, the temperatures of the wall and of the fluid must be known.

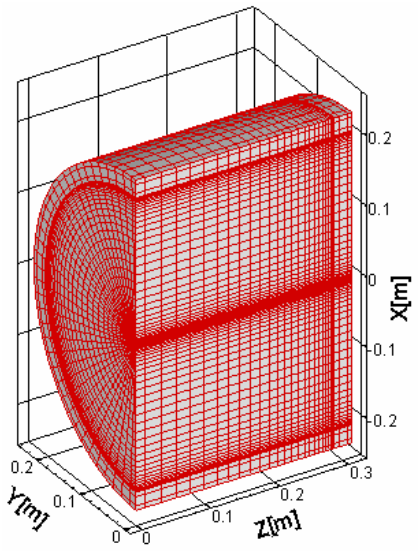

Figure 3 – Discretized calculation domain.

Considering that the temperatures of the wall and of the fluid vary according to height, it is necessary to define a reference value for each of these temperatures. The following relationships were applied to the calculation domain:

$$\overline{T}_{mw=} \frac{\sum_{i=1}^{L}\sum_{k=1}^{N} T\left(\theta_i^*, R_{\text{int}}, z_k\right)\cdot \Delta z_k \cdot \Delta A_i + \sum_{i=1}^{L}\sum_{j=1}^{M} T\left(\theta_i^*, r_j, Z_{\text{int}}\right)\cdot \Delta r_j \cdot r_j \Delta\theta_i \cdot Z_{\text{int}}}{\sum_{i=1}^{L}\sum_{k=1}^{N} \Delta z_k \cdot \Delta A_i + \sum_{i=1}^{L}\sum_{j=1}^{M} \Delta r_j \cdot r_j \Delta\theta_i \cdot Z_{\text{int}}} \tag{1.7}$$

$$\overline{T}_f = \sum_{i=1}^{L}\sum_{j=1}^{M}\sum_{k=1}^{N} T(\theta_i^*, r_j^*, z_k^*)\cdot r\Delta\theta_i \cdot \Delta r_j \cdot \Delta z_k \tag{1.8}$$

where $\overline{T}_{mw}$ and $\overline{T}_f$ are, respectively, the mean temperature of the metallic wall and the mean temperature of the fluid. After $\overline{T}_f$ and $\overline{T}_{mw}$ were defined, the number of Rayleigh was calculated as $Ra = \frac{g\beta R_{\text{int}}^3\left(\overline{T}_f - \overline{T}_{mw}\right)}{\upsilon\alpha}$. The symbol θ^* is used for the mean angle between the angles θ_i and θ_{i+1}, that is, $\theta_i^* = \frac{\theta_{i+1}+\theta_i}{2}$. θ^* corresponded to the mean point of the control volume, whereas θ indicates the boundaries of this volume. Hence, $\Delta\theta_i = \theta_{i+1} - \theta_i$. Due to the vertical stratification of the temperature field of the horizontal cylinder, the calculation of the mean temperature of the radial wall is weighed with the volume of the fluid layer located at the same height of the area element of the metallic wall, as shown in Fig. 4. Hence, for the segment $\Delta\theta_{i+1} = \theta_{i+1} - \theta_i$, the temperature $T(\theta_i^*, R_{\text{int}}, z_k)$ is weighed with the volume $\Delta A_i \Delta z_k = \left[A\left(\theta_{i+1}\right) - A\left(\theta_i\right)\right]\Delta z_k$.

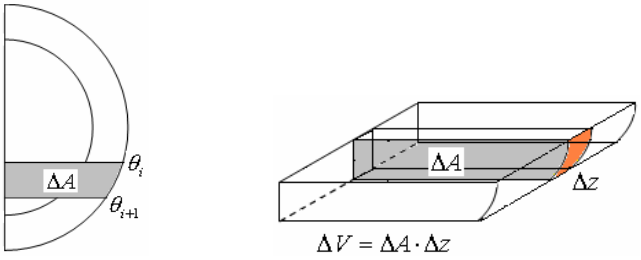

Figure 4 – Volume of the fluid layer located at the same height of the area element of the metallic wall.

The same criterion is used for the calculation of the mean temperature of the axial wall, where the temperature $T(\theta_i^*, r_j, Z_{\text{int}})$ is weighed with the volume $r_j \Delta\theta_i \Delta r_j Z_{\text{int}}$.

This procedure of the mean weighed with the volume is necessary in order to avoid overestimation the temperature of the wall of the base of the tank, as it is significantly lower than mean temperature of the fluid in the tank, but it is horizontally neighboring a small portion of the fluid. In order to weigh the radial wall temperature with the adjacent fluid temperature, the following formula, obtained by analytical integration, is used to calculate the transversal section area (and consequently ΔA increase):

$$A(\theta) = R_{\text{int}}^2 \left(\theta - \frac{\pi}{2}\right) + \frac{R_{\text{int}}^2 sen\left(\theta - \frac{\pi}{2}\right)\cos\left(\theta - \frac{\pi}{2}\right)}{2} + \frac{\pi R_{\text{int}}^2}{4} \tag{1.9}$$

For the calculation of the Nusselt number, the global coefficient of heat transference (U) as:

$$U = \frac{1}{R_{tot} A} \tag{1.10}$$

where total thermal resistence (R_{tot}) is determined by the relationship

$$R_{tot} = \frac{\bar{T}_f - T_\infty}{Q} \tag{1.11}$$

Heat transfer rate in the radial (Q_{rad}) and axial directions (Q_{axi}), respectively, are numerically calculated by the relationships:

$$Q_{axi} = k_{ins} \int_0^{\pi} \int_0^{Z_{ext}} \left.\frac{\partial T}{\partial r}\right|_{r=R_{ext}} dz r d\theta \tag{1.12}$$

$$Q_{rad} = k_{ins} \int_0^{\pi} \int_0^{R_{ext}} \left.\frac{\partial T}{\partial z}\right|_{z=Z_{ext}} dr\, r d\theta \tag{1.13}$$

Hence, the global coefficient of heat transfer at the radial and axial boundaries are $U_{ext_{rad}} = \frac{1}{R_{tot_{rad}} A_{ext_{rad}}}$ and $U_{ext_{axi}} = \frac{1}{R_{tot_{axi}} A_{ext_{axi}}}$. Therefore, the Nusselt number for the radial and axial boundaries can be determined by

$$Nu = \frac{U_{ext} R_{ext}}{k} \tag{1.14}$$

where k is air thermal conductivity.

3. Numerical Results

When the cooling process starts, it is observed that the formation of the thermal and hydrodynamic boundary layers, which are responsible for the formation of the stratified profile of the temperatures in the vertical plans. In the beginning, the hydrodynamic boundary layer extends until the bottom of the tank. As time passes, and the stratified profile of temperatures develops, the fluid cools near the walls at the superior area of the tank no longer descends to the bottom of the tank, but rather to an intermediate position. This position corresponds to a point where the temperature of the cooled fluid is equivalent to the mean temperature of the fluid in a horizontal plan.

Figure 5a shows the temperature field at the boundary of the fluid with the metallic wall, and Figure 5b shows the temperature fields of the symmetry plans after 1 hour of cooling. It can be seen that the temperature field is highly stratified at the bottom of the tank, whereas temperature is virtually constant at the top of the tank. The lateral view (Fig. 5a) shows that, for a determined horizontal plan, a thin layer of fluid, which temperature is lower than the mean temperature of this plan, is formed closed to the tank wall due to heat loss to the outside, i.e., a thermal boundary layer is formed. At the symmetry plans (Fig. 5b), temperature profiles at a determined height are virtually constant, except close to the walls, where the thermal boundary layer is formed. Figure 4a also shows small temperature fluctuations, particularly at the highest region of the tank, due to three-dimensional hydrodynamic instabilities, as well as more fluid cooling in the region close to the region where the radial and the axial walls meet. This is explained by the fact that the area of heat exchange with the outside in this region is larger because the fluid is in contact with both walls (radial and axial).

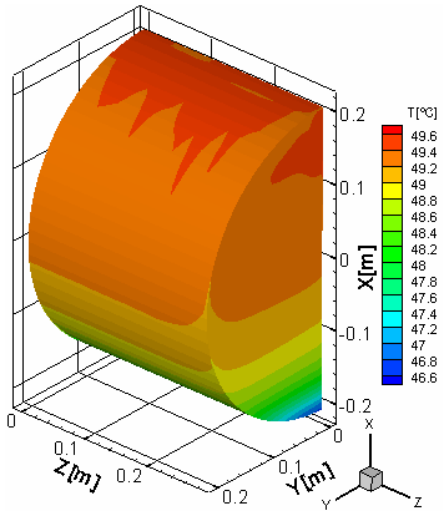

Figure 5a – Temperature field at the boundary of the fluid with the metallic wall.

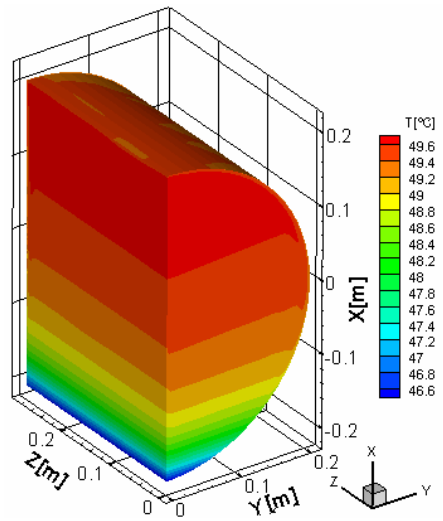

Figure 5b – Temperature fields of the symmetry plans.

Figure 6 shows the vertical profiles along the diameter, at the intersection of the symmetry plans, for a period of 10 hours of simulation.

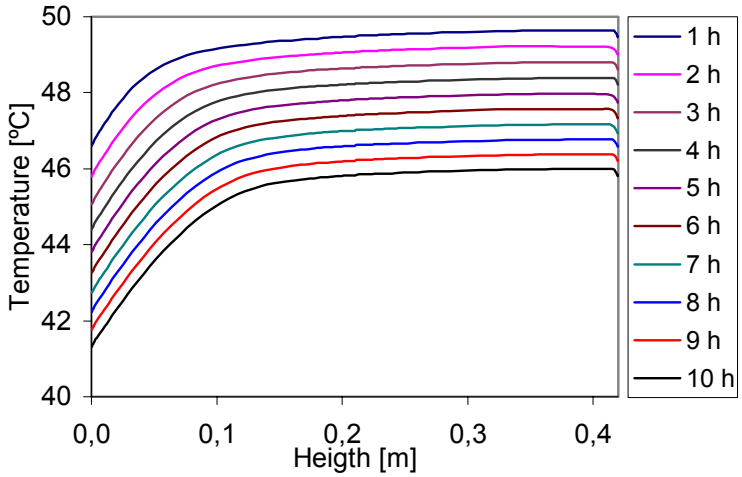

Figure 6 – Temperature profiles along the intersection of the symmetry plans.

It is observed that the stratification profile assumed after one hour is kept almost unchanged during the next hours, with the highest gradients occurring at the bottom of the tank. However, the difference between the maximum and the minimum temperature inside the tank increased from 3.2ºC to 4.5ºC between the first and the 10th hour.

Figure 7a and 7b present two cross sections of the plan (r, θ), showing the respective velocity components (V_r, V_θ) through the vectors. Figure 7a corresponds to the cross section near the axial wall, and Fig. 7b corresponds to a cross section in the middle of the tank. Figure 7a shows that the cooled fluid flows vertically. This cross section, located 5 mm from the axial wall is inside the hydrodynamic boundary layer by this wall. In addition, it is observed that the descending movement of the fluid is more intense. This region is close to both radial and axial walls, and therefore looses heat to both boundaries, suffers a more effective cooling, causing a more intense movement of the descending fluid. Figure 7b corresponds to a cross section located far from the axial lids, and shows that the fluid is cooled only by the radial wall, and hence the fluid movement mainly accompanies the outline of this wall. A secondary re-circulation is also seen in the highest region of the tank. The analysis showed that such re-circulations are transiently developed in the entire interior region of the tank.

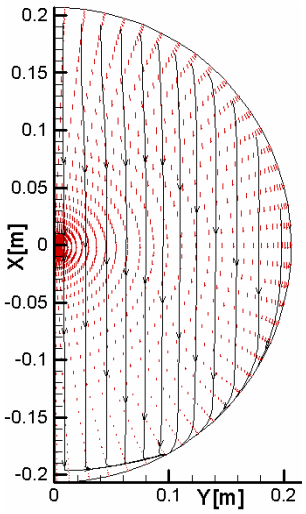

Figure 7a – Velocity components (V_r, V_θ). Cross section near the axial wall.

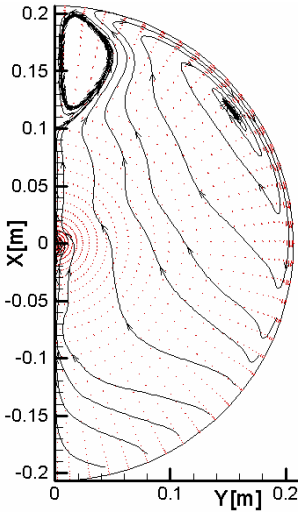

Figure 7b – Velocity components (V_r, V_θ). Cross section in the middle of the tank.

The analysis of the transient aspect of the three-dimensional velocity field demonstrated that preferential paths are formed, which shapes the velocity profile close to the radial wall in the direction of the z-axis as "fringes", as seen in Fig. 8a, which shows cross sections of the velocity fields at some fixed heights. In Fig 8b, cross sections of the velocity fields of some angular values are shown. Again, the formation of the thermal boundary layer by the radial and axial walls, as well as the formation of re-circulations at the top of the tank is also observed.

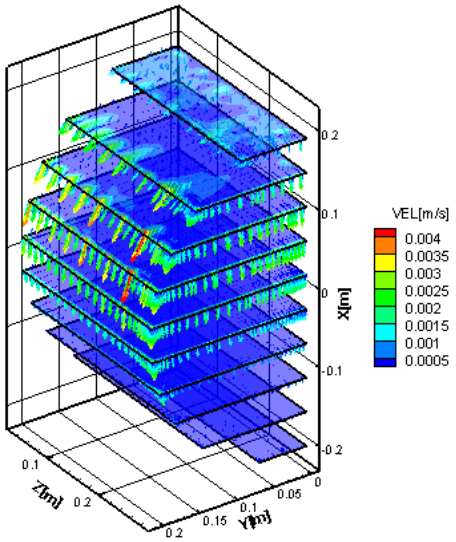

Figure 8a – Cross sections of the velocity fields of some fixed heights.

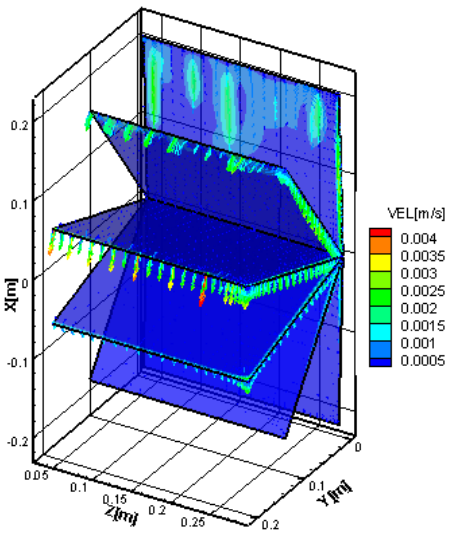

Figure 8b – Cross sections of the velocity fields of some angular values.

Such flow behaviors are according to the results of other researchers. For example, in an experimental investigation of natural convection in horizontal cylindrical tank, Brooks and Ostrach (1969) verified that the flow occurs mainly in the regions that are closer to the walls. Xia *et al* (1998), in their numerical and experimental study, concluded that this flow close to walls determines temperature stratification.

Figure 9 shows the evolution of mean temperatures of the wall (T_{mw}) and of the fluid (T_f) during 10 hours of simulation as calculated by Eq. 1.7 and 1.8. It can be observed that the mean wall temperature is slightly lower than the mean fluid temperature. Moreover, this difference slowly decreases as the tank cools. For instance, $\Delta T = 0{,}187°C$ after 1 hour, and $\Delta T = 0{,}158°C$ after 10 hours. For the case studied here, considering the 10-hour interval, the number of Rayleigh, according to definition above, was $0{,}8 \cdot 10^5 \leq Ra \leq 1{,}0 \cdot 10^5$, showing that the movement of the fluid inside the tank due to natural convection can be defined as laminar. During the simulated time interval, the Nusselt number for the

radial and axial boundaries had similar behavior, with a slight decrease along the time interval, as seen in Fig. 10. Moreover, it was verified the Nusselt number for the axial boundary us lower than that for the radial boundary due to the stratification profile of the fluid inside the tank, which causes the heat flow in the radial direction to be higher than the heat flow in the axial direction.

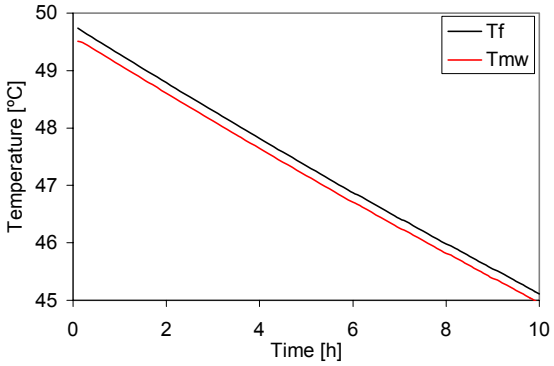

Figure 9 – Variation of the mean temperatures of the fluid (T_f) and of the metallic wall (T_{mw}) along 10 hours.

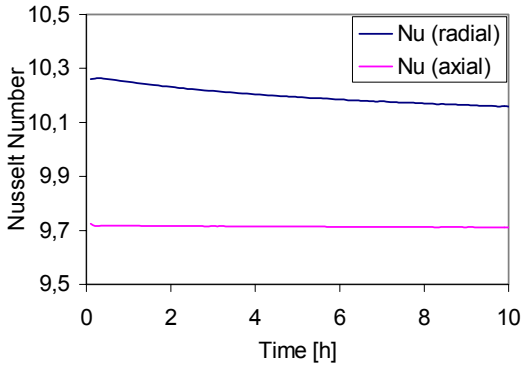

Figure 10 – Variation of the Nusselt number for the radial and axial boundaries along 10 hours.

4. Conclusions

This study developed a computational code for a three-dimensional simulation of the laminar natural convection, which was used to investigate a case of heat transfer in a horizontal cylindrical thermal tank with boundary condition of the third kind. Using a 40 x 40 x 40 grid (r, θ, z), the calculations were carried out within acceptable computational time. It was verified that the thermal and hydrodynamic boundary layers presented three-dimensional fringed shaped instabilities, particularly close to the radial wall. It was also verified that occurs primary recirculation close to the walls of the storage tank, caused by the cooling of the fluid, as well as the formation of transient secondary recirculations in the upper region of the storage tank. As occurs in vertical cylindrical tanks, there is also vertical temperature stratification in the horizontal cylindrical tank during the cooling process. The results show that, due to the characteristics of this stratification profile, average heat flow through the axial wall is slightly lower than that on the radial wall, implying in a lower axial Nusselt number.

5. References

Brooks, I., Ostrach, S., 1970. “An Experimental Investigation of Natural Convection in a Horizontal Cylinder”, Journal of Fluid Mechanics, Vol. 44, pp. 545-561.

Oliveski R.C., Vielmo H.A., Krenzinger, A., 2003. “Cooling of Cylindrical Vertical Tanks Submitted to Natural Internal Convection”, International Journal of Heat and Mass Transfer, Vol. 46, pp 2015-2026.

Patankar, S.V., 1975, “Numerical Prediction of Three-Dimensional Flows”, B.E. Launder (ed.), Studies in Convection: Theory, Measurement and Applications, Vol. 1, Academic, New York.

Rubinov A. et al, 2004. “Three-Dimensional Instabilities of Natural Convection Flow in a Vertical Cylinder With Partially Heated Sidewall”, Journal of Heat Transfer, Vol. 126, pp 586-599.

Schneider S., Straub, J., 1992. “Laminar Natural convection in a Cylindrical Enclosure with Different End Temperatures”, International Journal of Heat and Mass Transfer, Vol 35, pp 545-557.

Xia J. L. et al, 1998. “Numerical and Experimental Study of Transient Turbulent Natural Convection in a Horizontal Cylindrical Container”, International Journal of Heat and Mass Transfer, Vol 41, pp 3635-3645.

6. Responsibility notice

The authors are the only responsible for the printed material included in this paper.

7. Aknowledgements

This work has been developed under the sponsorship of the Conselho Nacional de Desenvolvimento Científico e Tecnológico – CNPq, Brazilian government entity for scientific and technology development.